Research

Late-Season Decline: A New Bacterial Disease of Corn Identified in the Texas Panhandle

Ken Obasa,[1,†] Michael Kolomiets,[2] Blayne Reed,[3] Dennis Coker,[4] Jourdan Bell,[5] and Kevin Heflin[5]

[1] Department of Plant Pathology and Microbiology, Texas A&M AgriLife Research and Extension Center, Amarillo, TX 79106
[2] Department of Plant Pathology and Microbiology, Texas A&M University, College Station, TX 77843
[3] Department of Entomology, Texas A&M AgriLife Extension Services, Plainview, TX 79072
[4] Department of Soil and Crop Sciences, Texas A&M AgriLife Extension Services, Dumas, TX 79029
[5] Department of Soil and Crop Sciences, Texas A&M AgriLife Research and Extension Center, Amarillo, TX 79106

Accepted for publication 9 January 2023.

Abstract

The genus *Pantoea* has historically been associated with two diseases of corn, Stewart's wilt caused by *P. stewartii* and necrotic or white leaf spots or streaks and stalk rot caused by *P. ananatis*. In 2020 and 2021, a sudden and unusual decline of corn stands was observed in corn fields in two counties in the Texas High Plains region. Symptoms observed included initial light green, elongated, slightly translucent, and nonchlorotic streaked lesions with nonwavy margins that developed on leaf blades during corn vegetative growth stages, with lesions becoming necrotic at the onset of crop reproduction. Additionally, stunting of affected plants, poor ear development, and stalk rot were associated with affected stands. Diagnosis of symptomatic tissues consistently recovered bacteria. BLAST searches of the partial 16S rRNA sequences of the bacterial isolates identified them as belonging to the genus *Pantoea*. Investigations of the pathogenicity of two bacterial isolates, B566 and B623, under greenhouse conditions relying on Koch's postulates resulted in the development of symptoms identical to those observed on symptomatic field corn plants. The two bacteria were also successfully recovered from symptomatic leaf and stem tissues, thus satisfying Koch's postulates. Sequence analysis showed that these isolates are closely related to *P. ananatis* but also phylogenetically distinct. The findings from this study provide evidence for a new disease of corn caused by two *Pantoea* species that can result in stand decline of infected corn plants.

Keywords: bacteriology, corn, plant pathology

Corn (*Zea mays* L.) is the most important agricultural crop in the United States based on production volume, with a 2017 production value of $49.5 billion from a total of 36.5 million hectares (USDA National Agricultural Statistics Service, 2017 Census of Agriculture. Complete data available at www.nass.usda.gov/AgCensus). In Texas, fungi are the most common causes of corn diseases. However, during the 2021 cropping season, sudden, drought stress-like symptoms developed on previously green and healthy corn stands in a fungicide trial study at the Texas A&M AgriLife Experiment Station at Bushland, Texas (Fig. 1). The study comprised a total of 100 plots, including the nontreated control plots, and measured 12.5 m^2 each. Initial symptoms consisted of light green, elongated, slightly translucent, and nonchlorotic streaked lesions with nonwavy margins that developed on the leaf blades during corn vegetative growth stages (Fig. 2A). Under wet or humid conditions, such as after rain or irrigation, water-soaked margins were occasionally observed around the margins of the lesions. Later in the season, at the onset of the reproductive stage of growth (VT), the incidence and severity of the symptoms increased significantly. During this time, the foliar lesions often enlarged, coalesced, and became necrotic, resulting in leaf blight symptoms that progressed from the leaf tips toward the base of affected leaves. Infected plants also often exhibited stunted growth (Fig. 2B). During this phase of symptom development, affected plants appeared drought stressed. Other symptoms observed on affected plants included arrested ear development (Fig. 2C), with incompletely developed ears occasionally decomposing (Fig. 2D), and small and poorly developed corn ears with few or no kernels (Fig. 2E). Stalk rot is also associated with affected plants (Fig. 2F and G). Lodging of affected plant stands was also correlated with incidences of stalk rot in the affected plants (Fig. 2H). Overall, yield loss from the affected field averaged about 93%. Disease development spanned all of the study plots, treated and nontreated plots alike. Diagnosis of symptomatic plant tissues from both the early and later stages of symptom development for a potential causal organism frequently resulted in the isolation of bacteria, and in several cases no fungi, on culture media. Preliminary investigations of the identity of the two isolated bacteria, following single-colony purification (details below), through BLASTN searches of their partial 16S rRNA sequences indicated that they were most closely related to *Pantoea ananatis*. The observed foliar symptoms, however, are distinct from those caused by *P. ananatis* in corn, which results in necrotic or white leaf spots or streaks (Bomfeti et al. 2008; Krawczyk et al. 2021; Paccola-Meirelles et al. 2001) and stalk rot (Goszczynska et al. 2007).

[†]Corresponding author: K. Obasa; ken.obasa@ag.tamu.edu

Funding: Funding was provided by the Texas Corn Producers Board (M2201531).

The author(s) declare no conflict of interest.

© 2023 The American Phytopathological Society

Pantoea ananatis was first identified and reported as a plant pathogen causing fruitlet rot of pineapple in the Philippines (Serrano 1928). It has since been designated as an emerging pathogen because of its increasing numbers of previously unreported hosts, including as a pathogen of corn; Palea browning (or dark brown leaf lesions) and stalk rot disease of rice (Cother et al. 2004); sudangrass leaf blotches and streaks (Azad et al. 2000); onion leaf blight, seed stalk rot, and bulb decay (Gitaitis and Gay 1997); wheat brownish leaf lesion (Krawczyk et al. 2020); and tomato gray wall disease (Stall et al. 1969). Symptoms of *P. ananatis* infection of corn are distinct from those of Stewart's wilt (Roper 2011), caused by *Pantoea stewartii*. Symptoms of Stewart's wilt include water-soaked light green lesions with necrotic centers and wavy and chlorotic margins that run parallel to the leaf veins (Roper 2011).

Subsequent to these initial observations of symptoms of a potentially new corn disease, identical foliar symptoms were observed on corn plant samples from Potter County submitted to the Texas High Plains Plant Disease Diagnostic laboratory, located in Amarillo, Texas, for disease diagnosis. Bacteria closely related to *P. ananatis*, on the basis of their respective 16S rRNA partial sequences, were recovered from all diseased samples. In 2021, widespread lodging attributed to stalk rot was observed in a grower's irrigated corn field that resulted in a loss of 4.4 to 5.7 thousand kg/ha. *Pantoea* sp. closely related to *P. ananatis* on the basis of 16S rRNA was similarly recovered from affected plant stands. Then, in 2022, identical symptoms were observed in growers' corn fields in seven additional counties in the Texas Panhandle, specifically in Dallam, Hartley, Sherman, Moore, Hutchinson, Hansford, and Oldham counties. Diagnosis of diseased plants identified during surveys of and visits to suspect fields also recovered bacteria belonging to the genus *Pantoea*. BLASTN searches of the partial 16S rRNA resulting sequences indicated that the new isolates were closely related to *P. ananatis*. Sequence alignments of the 16S rRNA sequences of isolates from 2021 and 2022 shared nucleotide identities ranging between 98.7 and 100% (data not shown). Disease severity, however, varied across the affected fields in the different counties. Because neither *P. stewartii* nor any other previously reported corn bacterial pathogens were recovered from symptomatic tissues, the objective of this study was to investigate the pathogenicity of the newly recovered bacterial isolates.

FIGURE 1

Field-grown corn in 2021 during the **A,** vegetative growth stage (V5-V7) showing no disease symptoms, **B,** a section of the field, and **C,** partial field view during the dough/dent growth stage (R4/R5) showing severe foliar blight and drought-like symptoms of the late-season decline disease on corn plants.

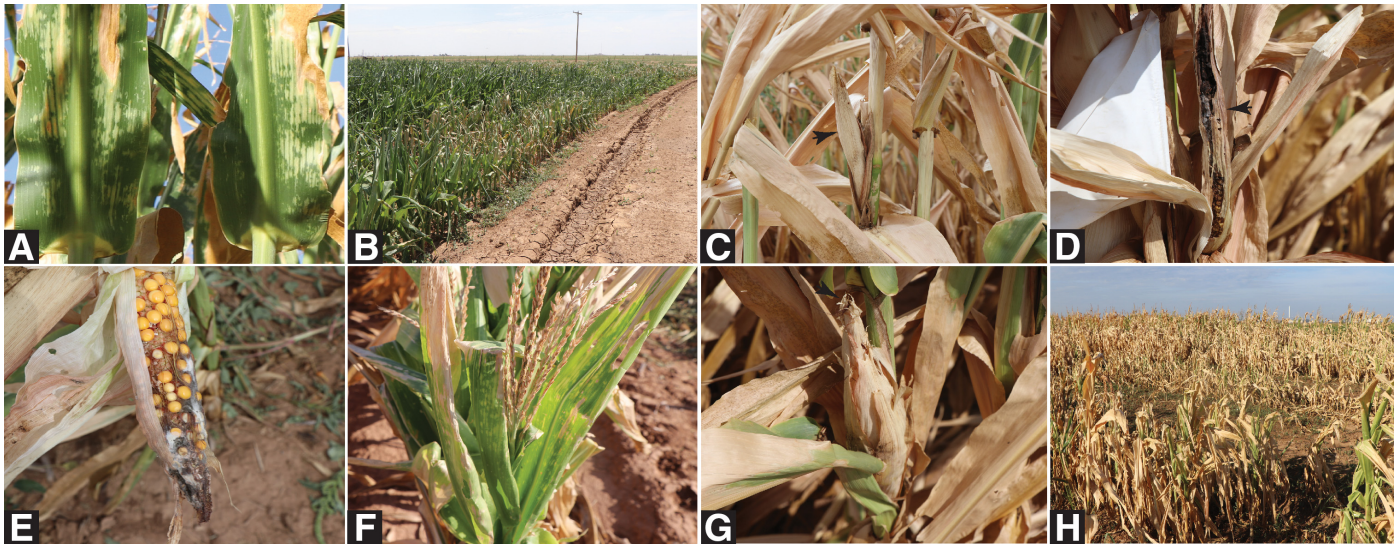

FIGURE 2

Symptoms of the late-season decline disease on field corn plants including **A,** pale-green foliar lesions and blight, **B,** stunting, **C,** poorly developed and **D,** unfertilized corn ears, **E,** hypertrophied kernels, **F,** tassel senescence, **G,** silk rot and abscission, and **H,** stalk rot-induced lodging.

Materials and Methods

Bacterial isolations, purification, and identification

Symptomatic corn leaf and stem tissues from naturally infected field corn plants or inoculated greenhouse plants were rinsed in sterile-distilled water and surface sterilized by soaking in 10% hypochlorite solution for 1 min, then rinsed in five changes of sterile double-distilled water. The surface-sterilized leaf and stem tissues were blotted dry on Kimwipes (catalog #34155; Kimberly-Clark, Roswell, GA) and cut into 0.5 to 1 cm-long sections with sterile scalpel blades. The cut tissue sections were placed in Petri dishes containing water agar using sterile forceps, and the plates were incubated in the dark at 25°C. Following the incubation period, bacterial and fungal outgrowths from the sectioned tissue samples were purified through sequential subculturing steps. The bacteria were single-colony purified by streaking onto Luria Bertani (LB) agar plates and incubated overnight in the dark at 28°C. Representative colonies from the resulting single colonies were selected and further purified through a second round of streaking on LB agar plates and similarly incubated overnight. The plates were subsequently incubated at 25°C in the dark. Single round and yellowish bacterial colonies with smooth margins from the second purification round were transferred separately into LB broth and incubated overnight at 28°C and 240 rpm. Genomic DNA was extracted, as previously described by Maniatis et al. (1982), from the overnight cultures and used in downstream analysis. The 16S rRNA polymerase chain reaction (PCR) amplification was carried out using the primer pair 27F (AGAGTTTGATCMTGGCTCAG) and 1492R (GGTTACCTTGTTACGACTT) (Galkiewicz and Kellog 2008) at a final concentration of 0.5 µM and 1× final concentration of Bio-Rad 2× HF Master Mix (BIO-RAD, Hercules, CA) in a 25 µl total reaction volume. The PCR amplification cycle consisted of an initial denaturing step at 98°C for 3 min; 35 cycles of three steps consisting of 98°C for 10 s, 57°C for 30 s, and 72°C for 30 s; and a final step of 72°C for 10 min. The PCR products, ~1,500-bp amplicons, were sequenced, and the resulting sequences were used to identify the respective bacteria through BLAST searches.

Whole-genome sequencing and alignments

DNA library preparation and sequencing. Bacterial DNA library preparation and sequencing for two representative bacterial isolates, B566 and B623, were carried out as described by Obasa and Haynes (2022). For Illumina short-read sequencing, the genomic DNA of each sample was randomly sheared into short fragments of about 350 bp, which were used for library construction using the NEBNext DNA Library Prep Kit (New England Biolabs, Ipswich, MA) according to the manufacturer's instructions. This was followed by end repairing, dA-tailing, and ligation with the NEBNext adapter. The required fragments (300 to 500 bp size) were PCR enriched by P5 and indexed P7 oligos. The prepared DNA library was then purified and verified for concentration and quality using a Qubit 2.0 fluorometer and subsequently assessed for insert size using the Agilent 2100 bioanalyzer (Agilent Technologies, CA). Finally, the constructed libraries were pooled and paired-end sequenced on the Illumina HiSeq (Illumina, San Diego, CA) sequencing platform. For long-read sequencing with Oxford Nanopore MinION (Oxford Nanopore Technologies, Cambridge,

TABLE 1
List of 25 bacterial species and genes used for multilocus sequence comparisons and phylogenetic analysis of *Pantoea* sp. isolate B566 and *Pantoea* sp. isolate B623

		Gene locus tag					
Organism	**Accession**	***dnaK***	***fumC***	***gyrB***	***murG***	***trpB***	***tuf***
Pantoea sp. B566	JANUQL000000000	NYE92_18315	NYE92_03155	NYE92_15010	NYE92_18590	NYE92_04380	NYE92_15695
Pantoea sp. B623	JANUXM000000000	NXS97_09795	NXS97_03250	NXS97_12875	NXS97_09520	NXS97_02005	NXS97_14930
Pantoea sp. B270	JAHCSX000000000	KOL70_20725	KOL70_04545	KOL70_12235	KOL70_15690	KOL70_05705	KOL70_10780
P. ananatis LMG2665 [T]	GCA_000710035	CM04_RS0100395	CM04_RS0106720	CM04_RS0123440	CM04_RS0100685	CM04_RS0108220	CM04_RS0119540
P. dispersa BJQ0007	CP045216	GAY20_03220	GAY20_11875	GAY20_00020	GAY20_17200	GAY20_10790	GAY20_01460
P. dispersa DSM 32899	CP032702	D8B20_03060	D8B20_08045	D8B20_00025	D8B20_03295	D8B20_09210	D8B20_00950
P. cypripedii NE1	CP024768	CUN67_03105	CUN67_08795	CUN67_20310	CUN67_03350	CUN67_10795	CUN67_18450
P. stewartii ZJ-FGZX1	CP049115	G5574_16850	G5574_01360	G5574_13485	G5574_17090	G5574_02770	G5574_11725
P. stewartii subsp. *indologene* LMG 2632 [T]	GCA_000757405.2	HA47_13145	HA47_17800	HA47_00680	HA47_13390	HA47_19855	HA47_18510
P. vagans FDAARGOS_160	CP014129	AL522_07335	AL522_13560	AL522_04680	AL522_07575	AL522_14765	AL522_05425
P. vagans C9-1	CP002206	PVAG_0071	PVAG_1259	Pvag_3306	PVAG_0121	PVAG_1508	PVAG_2894
Pantoea sp. SM3640	CP064872	IV493_14975	IV493_09115	IV493_17640	IV493_14725	IV493_07900	IV493_01185
P. vagans FBS135	CP020820	B9D02_16265	B9D02_10490	B9D02_00020	B9D02_16025	B9D02_09315	B9D02_02080
P. agglomerans ASB05	CP046722	PAASB05_15965	PAASB05_10050	PAASB05_00020	PAASB05_15720	PAASB05_08815	PAASB05_02035
P. agglomerans AR1a	CP059089	H0Z11_17610	H0Z11_11655	HOZ11_01190	H0Z11_17360	H0Z11_10295	H0Z11_03260
Citrobacter sp. TBCP-5362	CP040234	FD428_18180	FD428_11550	FD428_00020	FD428_17795	FD428_10310	FD428_01930
Enterobacter cloacae SDM	NC_018079	A3UG_RS03495	A3UG_RS09980	A3UG_RS00020	A3UG_RS03780	A3UG_RS13070	A3UG_RS21170
Leclercia sp. 29361	CP049786	G7090_03620	G7090_10210	G7090_00020	G7090_03930	G7090_12920	G7090_00935
L. adecarboxylata 707804	CP049980	G7098_01325	G7098_07680	G7098_20625	G7098_01725	G7098_10445	G7098_18390
L. adecarboxylata 16400	CP060824	H9S86_18945	H9S86_12455	H9S86_22020	H9S86_18550	H9S86_09250	H9S86_25330
Mixta gaviniae DSM 22758	CP026377	C2E15_04050	C2E15_10125	C2E15_00215	C2E15_04320	C2E15_11345	C2E15_02050
M. calida 5098PV	CP061511	IDH70_03570	IDH70_09985	IDH70_00020	IDH70_03840	IDH70_11085	IDH70_01770
Erwinia amylovora ATCC 15580	CP066796	JGC47_13930	JGC47_08410	JGC47_00020	JGC47_13695	JGC47_09225	JGC47_01250
E. sp. Ejp617	CP002124	EJP617_04000	EJP617_28690	EJP617_11400	EJP617_03510	EJP617_30240	EJP617_08690
E. pyrifoliae DSM 12163	FN392235	EPYR_00735	EPYR_01999	EPYR_03952	EPYR_00786	EPYR_01796	EPYR_00251
E. pyrifoliae Ep1/96	FP236842	EPC_06950	EPC_18520	EpC_36670	EPC_07430	EPC_16700	EPC_02410
Bacillus sp. 5B6	NZ_AJST00000000	MY7_2311	MY7_RS13965	MY7_RS17940	MY7_1406	MY7_RS09360	MY7_RS18600

MA), library preparation was carried out with the Rapid Barcoding Sequencing kit (SQK-RBK004) according to the manufacturer's instructions. Sequencing was done using the R9 flow cells according to the manufacturer's instructions.

Assembly and annotation of sequence reads. The generated raw reads from all sequencing outputs were processed to remove adapters and primers using the post-run processing software for the respective sequencing technologies. The processed reads were assembled using the default settings of the Geneious SPAdes DNA seq de novo assembler (Biomatters, San Diego, CA; Bankevich et al. 2012; Gurevich et al. 2013). The assembly was analyzed to identify prokaryotic genes using GLIMMER (Delcher et al. 1999); the identified prokaryotic genes were subjected to a BLAST search, and the gene ontology (GO) terms associated with hits obtained from the BLAST search were retrieved by mapping (Gotz et al. 2008). Next, Blast2Go annotation (Gotz et al. 2008) and InterProScan annotation (Jones et al. 2014) were independently run on the mapped assembly, and the resulting annotation results merged. A final round of annotation using EggNOG mapper version 1.0.3 with EggNOG 5.0.0 (Huerta-Cepas et al. 2019) for the functional annotation of

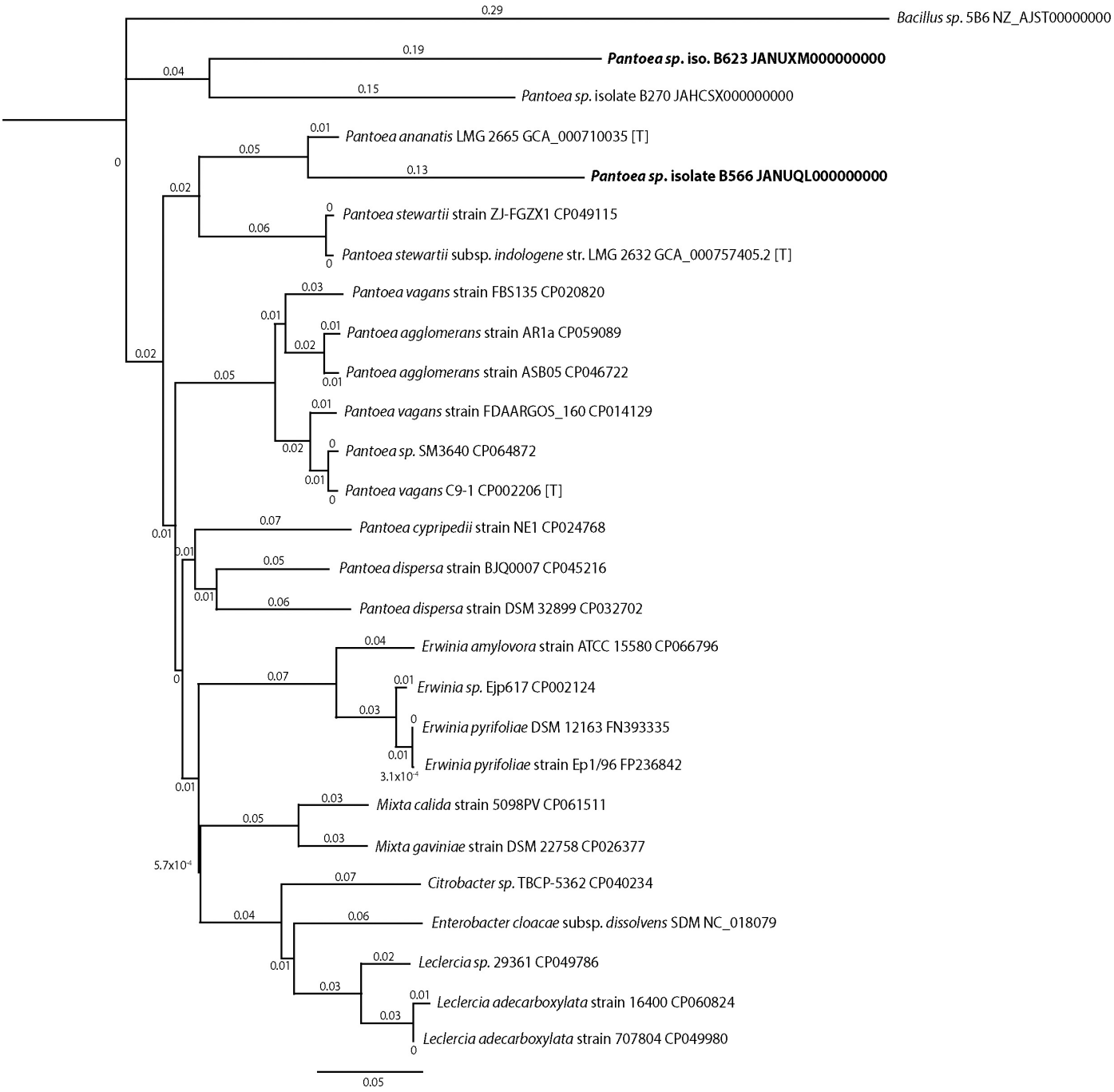

FIGURE 3

Phylogeny of *Pantoea* sp. B566 and *Pantoea* sp. B623 with 25 closely related species and an outgroup using concatenated sequences of six genes (*dnaK*, *fumC*, *gyrB*, *murG*, *trpB*, and *tuf*) showing their relatedness. Bar indicates branch length, estimated using the Tamura-Nei genetic distance model.

novel sequences using precomputed EggNOG-based orthology assignments was carried out, and the resulting annotations similarly merged with those from the earlier annotations.

Phylogenetic analysis. Multilocus sequence analysis using six genes (*dnaK*, *fumC*, *gyrB*, *murG*, *trpB*, and *tuf*) obtained from the respective draft genome sequences of two selected isolates, B566 and B62, was used for phylogenetic analysis. The sequences were concatenated and aligned to closely related species' similarly concatenated sequences (Table 1) identified using BLASTN (Altschul et al. 1990). A phylogenetic tree was constructed using the Tamura-Nei genetic distance model (Tamura and Nei 1993), using global alignment with free end gaps, a gap open penalty of 12, a gap extension penalty of 3, and a 65% similarity cost matrix for the pairwise alignment options for building a distance matrix available in the default settings of the Geneious Tree Builder application in Geneious Prime (Kearse et al. 2012). Furthermore, alignments of the respective assembled genomes of the corn bacterial isolates with those of the type strains of their respective closest relative identified by BLASTN were carried out using the JSpeciesWS online taxonomic threshold service (Richter et al. 2015; jspecies.ribohost.com/jspeciesws/#home) to determine the average nucleotide identity (ANI) between each pair.

Bacterial inoculum preparation

Bacterial cultures were grown overnight in LB broth at 28°C and 240 rpm. From the overnight cultures, a subculture was transferred into fresh LB broth and similarly incubated at 28°C and 240 rpm to an absorbance value (OD_{600}) of 0.5 as measured with the Denovix DS-11 FX + spectrophotometer (DeNovix, Wilmington, DE). To estimate the cell density in colony-forming units (CFU) for each bacterial culture, a subsample of the final culture was serially diluted in sterilized nuclease-free water (Ambion - Life Technologies, Austin, TX), spread on LB agar plates in triplicate, and incubated overnight in the dark at 28°C.

Pathogenicity assay of bacterial isolates on corn

Seeds of Pioneer corn hybrid "P1151" were planted in sterile potting media (Berger BM1 Nutrient Retention General Purpose Media; Hummert International, Topeka, KS) contained in 25-gallon plastic pots at the rate of four seeds per pot. The pots were lightly watered daily and maintained at 28°C, and a 14-h photoperiod was achieved with supplemental lighting under greenhouse conditions. Seventy-two days after germination, two randomly selected upper canopy leaves or stems were inoculated with the suspension of one of two randomly selected bacterial isolates, B566 or B623, at a final concentration of 7.5×10^6 CFU. Stem inoculation was done with 100 µl of bacterial suspension using a pipette. For leaf inoculation, either the leaf mid-rib was inoculated with 20 µl of bacterial suspension or the leaf lamina was inoculated with bacterial cells collected from single colony-purified cultures using the tip of a sterile toothpick to create up to 15 randomly distributed inoculation foci per inoculated leaf. All four plants in a pot were similarly inoculated, and two replicate pots per bacterial treatment were set up. Pots were arranged in a complete randomized design and observed for symp-

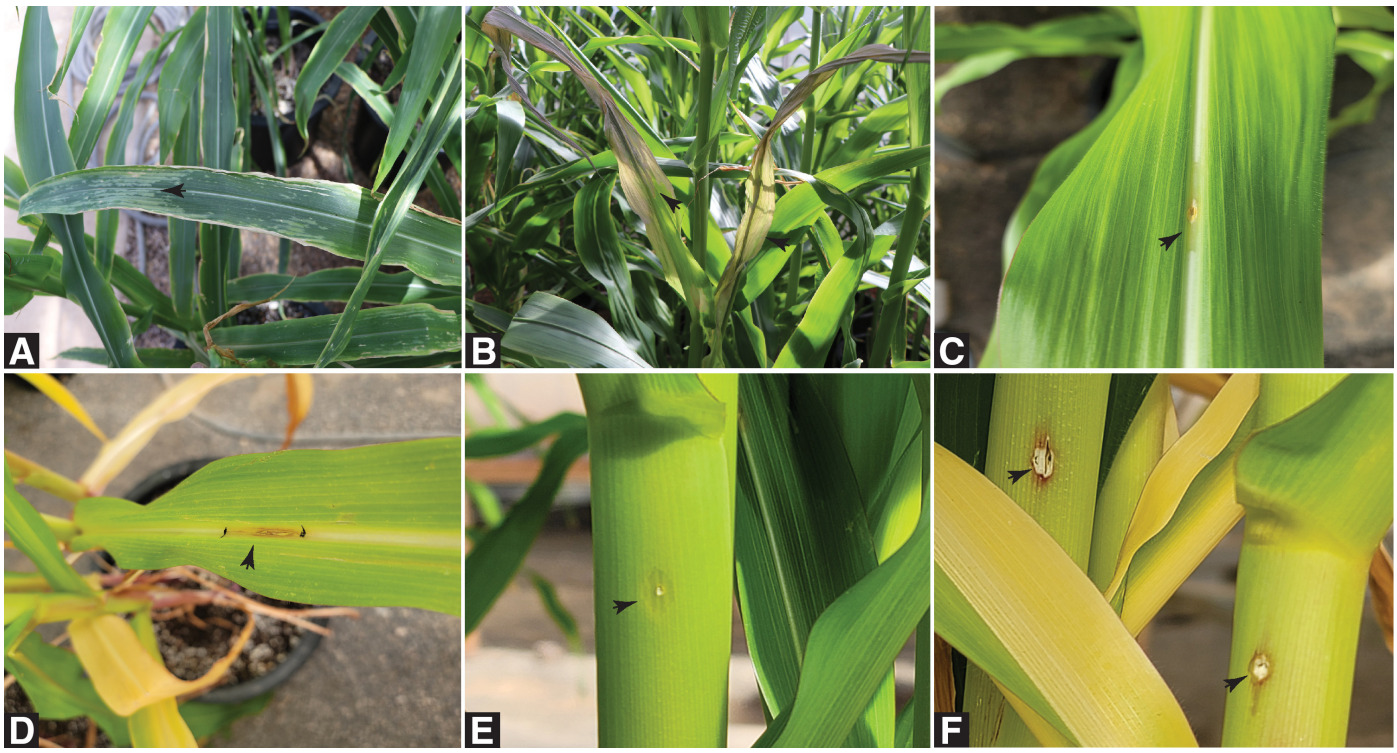

FIGURE 4

Koch's postulate evaluation of two bacterial isolates, B566 and B623, recovered from field corn plants affected by the late-season decline disease, under greenhouse conditions. Postinoculation pictures: **A,** the development of pale green foliar lesions (black arrow) during the vegetative growth stage, **B,** foliar blight (black arrow) after the onset of the reproductive growth stage, **C,** lesion with water-soaked appearance (black arrow) in inoculated leaf mid-rib during the vegetative growth stage and **D,** necrotized leaf mid-rib lesion (black arrow) after the onset of the reproductive growth stage, **E,** development of slightly sunken spherical stem lesion with water-soaked appearance (black arrow) during the vegetative growth stage that similarly became necrotic **F,** (black arrow) after the onset of the reproductive growth stage on inoculated plants.

tom development. Pots with plants similarly inoculated, but with sterile double-distilled water, in the stem, mid-rib, or leaf lamina with the tip of a sterile toothpick, served as the respective noninoculated controls. Following symptom development, representative tissues were collected and diagnosed to identify the causal pathogen. The collected symptomatic tissues were surface sterilized, placed on LB agar in Petri dishes, incubated, and subsequently diagnosed as described above for the presence of the bacteria used to inoculate the particular plant. Recovered bacteria were single-colony purified by streaking. The 16S rRNA sequence fragments from recovered bacterial isolates were aligned and compared with those of the bacterial isolates originally used to inoculate the respective plants. The study was conducted twice.

Results

Bacteria associated with symptomatic corn tissues

BLASTN searches of the 16S rRNA partial sequence of the bacterial isolates B566 (GenBank accession: OP268626) and B623 (GenBank accession: OP268628), as well as those of other recovered isolates from the field, determined that they all belong to the genus *Pantoea*, with *P. ananatis* (GenBank accession: MG681216.1, MK156144.1, and MK414947.1) identified as their most closely related species. Multilocus sequence analysis using six genes (*dnaK*, *fumC*, *gyrB*, *murG*, *trpB*, and *tuf*) obtained from the respective draft genome sequences of two selected isolates, B566 and B623, and phylogenetic analysis, however, indicated that bacterial isolate B566 is the most closely related to *P. ananatis* (Fig. 3). The analysis determined that B623 was most closely related to *Pantoea* sp. isolate B270 (GenBank accession: JAHCSX000000000), a recently discovered bacterial pathogen of peanut that causes bacterial early decline disease of peanut in Texas (Obasa and Haynes 2022). Nevertheless, the branching of the two bacteria indicated that they are in distinct genotype groups and likely represent unique species that are distinct from both *Pantoea* sp. isolate B270 and *P. ananatis* (Fig. 3). To further evaluate the relatedness of the two bacterial isolates, B566 and B623, with their closest relatives identified by the phylogenetic analysis, separate alignments of the whole-genome sequence of each bacterium with *Pantoea* sp. isolate B270 (GenBank accession: JAHCSX000000000), and a type strain of *P. ananatis* LMG 2665 (GenBank accession: GCA_000661975.1; Table 1) was performed. Additionally, the relatedness of B566 to B623 was assessed by conducting a whole-genome sequence alignment with a type strain of *P. stewartii* subsp. *stewartii* CCUG 26359 (GenBank accession: GCF_011044475.1; Table 1).

For the alignments of the genome of isolate B566 with those of *Pantoea* sp. B270, *P. ananatis* LMG 2665, and *P. stewartii* subsp. *stewartii* CCUG 26359, the calculated ANIs (and aligned nucleotide percentages) were 77.1 (61.9), 98.9 (89.4), and 83.6% (71.8%), respectively. For the alignments of the genome of isolate B623 with those of *Pantoea* sp. B270, *P. ananatis* LMG 2665, and *P. stewartii* subsp. *stewartii* CCUG 26359, the calculated ANIs (and aligned nucleotide percentages) were 77.1 (61.8), 98.8 (90.7), and 83.4% (71.9%), respectively. Additionally, the calculated ANI (and aligned nucleotide percentages) from the alignment of the genomes of isolates B566 and B623 was 98.8% (89.6%), indicating that isolates B566 and B623 are genetically distinct from each other, as well as *Pantoea* sp. B270, *P. ananatis*, and *P. stewartia*, respectively. Therefore, the two bacteria were designated *Pantoea* sp. isolate B566 (GenBank accession: JANUQL000000000) and *Pantoea* sp. isolate B623 (GenBank accession: JANUXM000000000).

Bacterial isolates pathogenic on inoculated corn plants

Inoculation of corn leaf margins with isolate B566 or B623 resulted in identical symptoms as those observed on affected field corn plants, including the development of light green, elongated, slightly translucent, and nonchlorotic streak lesions with nonwavy margins (Fig. 4A). Symptoms were initially quiescent, during the vegetative growth stage, but became active and necrotic from around the onset of tasseling (VT) (Fig. 4B). Inoculated mid-rib tissues de-

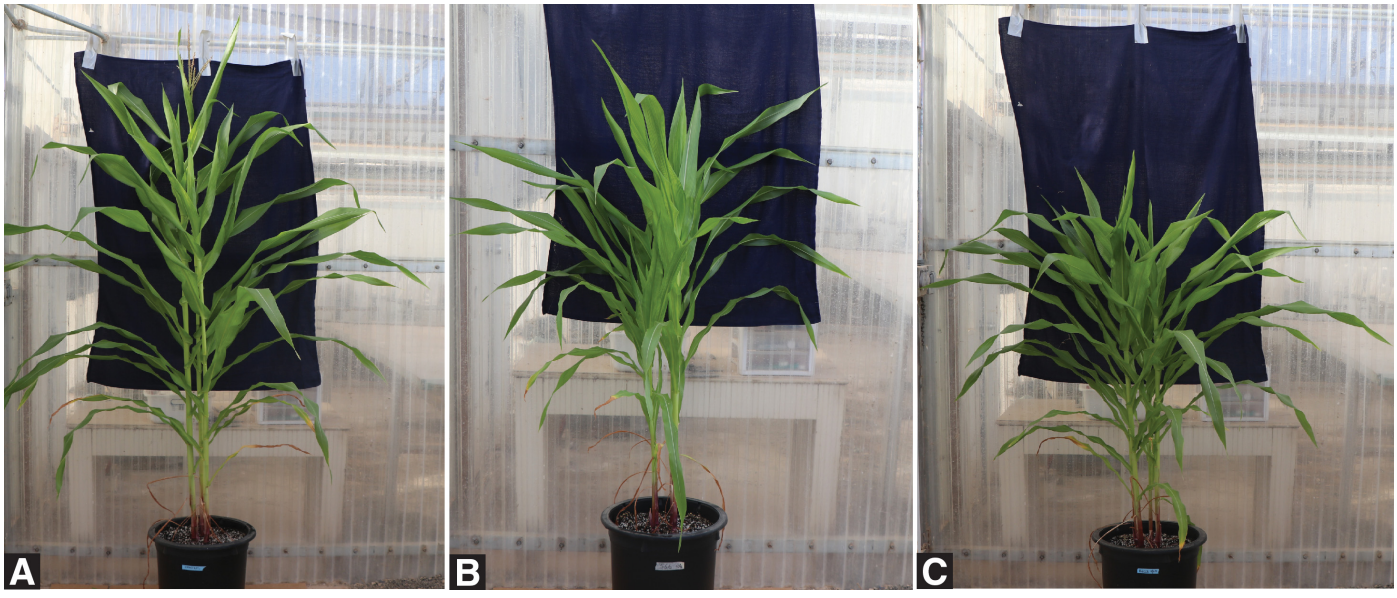

FIGURE 5

Koch's postulate evaluation of two bacterial isolates, B566 and B623, recovered from field corn plants affected by the late-season decline disease, under greenhouse conditions. Postinoculation pictures: **A,** normal growth of noninoculated control plants, and stunting and delayed onset of the VT growth stage in **B,** B566- and **C,** B623-inoculated plants.

veloped expanding water-soaked lesions around inoculation foci (Fig. 4C) that similarly turned necrotic around the VT growth stage (Fig. 4D). Plants inoculated through the stems also developed spherical, slightly sunken, and water-soaked lesions around inoculation foci (Fig. 4E), which also turned necrotic around the VT growth stage (Fig. 4F). Relative to the noninoculated control plants, all the stem-inoculated plants were also visibly stunted by the VT stage of growth, the onset of which was also delayed on the inoculated plants (Fig. 5). Stem pigmentation on inoculated plants (Fig. 6B and D) was visibly less compared with that on the noninoculated control plants around the dough to dent stage of growth (R4-R5) through maturity (Fig. 6A to D). Furthermore, at maturity, necrosis of vascular tissues extending from the inoculation foci was visible in stems of inoculated plants but not the noninoculated control plants (Fig. 6E and F). Finally, ears that developed on inoculated plants, relative to those on the noninoculated control plants, showed varying levels of malformation, ranging from poorly developed cobs to absence of kernels, as well as the presence of few and hypertrophied kernels on cobs (Fig. 7). Bacterial isolates recovered from leaf and stem lesions had 16S rRNA sequence identities that were 100% identical (data not shown) to those of the original bacterial isolates used to inoculate the respective plant tissues, thus satisfying Koch's postulates. Neither bacterium was recovered from the noninoculated plants.

Discussion

The discovery of symptoms of a new disease on corn plants, initially in Potter County, Texas, in 2020, and again in 2021, that affected leaves, stem vascular tissues, and ears and caused stunting led to the identification of bacteria belonging to the genus *Pantoea* as the causative agents of the disease. The initial identity of the bacterial pathogens was determined to be most closely related to *P. ananatis* based on the alignments of their respective 16S rRNA partial sequence fragments against those of closely related species identified through BLASTN searches of the National Center for Biotechnology Information database (https://blast.ncbi.nlm.nih.gov/Blast.cgi). Two isolates, B566 and B623, whose 787- and 624-bp 16S rRNA sequences respectively returned a 99.62 and 100% identity match with *P. ananatis* in BLASTN searches, were selected for further characterization, pathogenicity, and disease epidemiology studies. Whereas BLASTN analysis of the 16S rRNA sequences of bacterial isolates of the new corn disease identified *P. ananatis* as their closest relative, results of the MLSA and whole-genome sequence analysis suggest that the isolates of the new corn disease are genetically distinct from *P. ananatis* and could represent new species within the genus *Pantoea*. This distinction is also supported by the fact that the foliar symptoms of the new disease are phenotypically distinct from the necrotic spots and streak symptoms

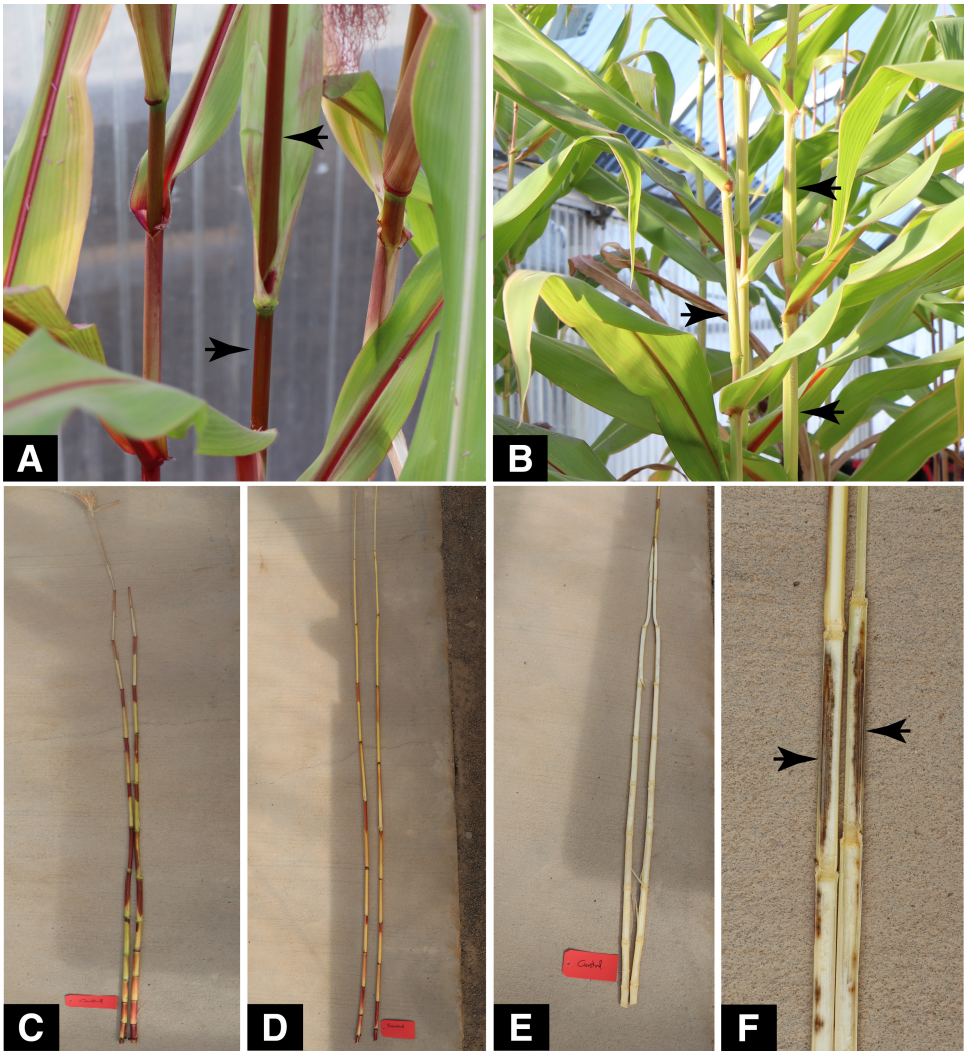

FIGURE 6
Comparison of the effect of stem inoculation on stem pigmentation shows **A and C,** conspicuous reddish pigmentation on the stem and leaf mid-ribs of noninoculated control plants and **B and D,** less prominent pigmentation of stems and leaf mid-ribs of inoculated plants. Longitudinal stem sections of **E,** noninoculated and **F,** inoculated plants showing the presence of stalk rot only in the stems of inoculated plants.

(Bomfeti et al. 2008; Krawczyk et al. 2021; Paccola-Meirelles et al. 2001) induced by *P. ananatis* in corn. This new disease is therefore designated bacterial late-season decline disease of corn (LSD). Overall, symptoms from inoculation of corn plants with the two bacterial isolates, B566 and B623, were identical to those observed on symptomatic corn plants in the field and included the light green, elongated, slightly translucent, and nonchlorotic streak lesions with nonwavy margins, stunting, and vascular necrosis, as well as small and poorly developed corn ears with few or no kernels that often were also hypertrophied. Foliar and stem lesions also became exacerbated and turned necrotic from around the onset of the reproductive growth stage. The onset of pigment development on stem in the hybrid used is associated with the period of increased stem lignification and ear development. The observed reduced stem pigmentation is therefore hypothesized to be related to the stalk rot induced by the bacteria in the stems of the inoculated plants. Additionally, although no lodging was observed during the two independent greenhouse studies, the stems of the inoculated plants at maturity were noticeably less rigid and prone to breaking when slightly leaned. The stem breakages were also observed to occur around the regions of the stems that had extensive stalk rot. A similar corn stand with stalk rot-induced weakened stems would be susceptible to lodging under the field conditions of often strong winds common in the Texas Panhandle, similar to observations of naturally infected field corn. The successful recovery of the two bacteria, B566 and B623, from the respective inoculated plants, but not from the noninoculated control plants, satisfied Koch's postulate and confirms that the bacteria induced the observed symptoms and, consequently, are the causative agents of the new disease. The fact that inoculations with isolates B566 and B623 resulted in identical symptoms, although their original source locations are about 116 miles apart in two separate counties (Potter and Hansford, respectively), further supports a causal role of these new *Pantoea* species in the disease development.

Following the first observed cases of the new disease in Texas corn in 2020 and again in 2021 in Potter and Hansford counties, in the Texas High Plains, the disease has since been confirmed in seven additional counties in 2022 in the Texas High Plains. Ongoing observations from investigations of suspected cases from corn fields in 2022 have revealed the occurrence of variations in the appearance of foliar symptoms in different corn hybrids, suggesting possible differential outcomes from host-pathogen interactions. Such interactions may or may not influence disease severity. However, it is noteworthy that the observed disease severity in 2022 varied across corn fields with different hybrids. In some fields, normal ear development did not appear to have been noticeably affected, along with minimal incidences of minor stalk rot, whereas in others, late-season foliar blight, evidence of abnormal ear development, and extensive stalk rots were observed. Factors such as the corn hybrid genotypes grown, ecological and local environmental conditions including weather, crop production, and pest management practices in the different fields could have been contributing factors. The rapid multicounty spread of the bacterial pathogen in the 12 months since the first confirmation of the disease in 2021 suggests the possibility of the existence of more than one mechanism of transmission of the causative bacteria. In the case of the disease outbreak that occurred in 2021 in the fungicide study plots at Bushland, Texas, the Pioneer P1151 corn hybrid seeds planted to the study plots were from the same seed batch that was used in previous field and greenhouse studies in 2019 and 2020, the two years immediately preceding 2021. In those studies, no instance of the disease was noticed, thus eliminating a seedborne origin in the particular Pioneer P1151 seed batch. The absence of the bacterial pathogens in the seed batch was also confirmed through seed testing (data not shown). Consequently, the 2021 disease outbreak likely resulted from pathogen introduction through a mechanism other than seed. Preliminary testing of a limited set of seeds from ears collected from two corn fields affected by the disease in 2021, however, successfully recovered bacteria whose 16S rRNA sequences showed high similarity to those of bacteria recovered from symptomatic leaf and stem tissues of the respective plants. BLASTN searches also identified *P. ananatis* as their closest relative (data not shown). Observations on this aspect have been inconsistent, and additional work is needed to elucidate any potential seed pathway in the spread of the disease bacterial pathogens.

Additional work is needed to determine sources of inoculum, transmission, and epidemiology of this new and rapidly spreading bacterial pathogen that has shown potential to cause significant economic losses. This is particularly important for Texas given that a substantial acreage of corn production is irrigated and thus can create a favorable microclimate for bacterial disease establishment.

FIGURE 7

Effect of inoculation on corn ear development shows **A,** normal ears from noninoculated control plants, whereas **B,** B566- and **C,** B623-inoculated plants produced poorly developed and deformed ears with few or no kernels, some of which were also hypertrophied.

If seed transmission is confirmed based on extensive seed testing in the future, the use of certified seed and preplanting seed treatment methods would be important for farmers to consider. It may also offer an opportunity for detection of potential seedborne inoculum through seed testing. This can help to identify infected seed lots for subsequent exclusion from trade and planting, as a way to limit the spread of the disease. Implementation of such a management strategy can help to mitigate the risk to farmers of the potential economic losses associated with the disease.

Conclusion

The findings from this work provide evidence for a new bacterial disease of corn that is distinct from previously reported bacterial diseases of corn. Although infection can become established early during the vegetative growth stage, disease severity increases during the reproductive growth stages of affected corn crops. The resulting foliar blight associated with symptom development during the reproductive growth stages, coupled with the potential to cause stalk rot, can adversely impact yield. Stalk rot-induced stand lodge, for instance, could reduce the harvestable ears, whereas foliar blight can limit the amount of photosynthate available for grain filling. The observations reported here indicate that the bacterial pathogen is able to spread quickly, suggesting that dispersal involves more than a single mechanism of transmission. Given the potential economic impact from the disease, and the absence of known resistant germplasm, elucidating the dispersal mechanism(s) will be very important toward safeguarding profitable corn production by farmers.

Literature Cited

Altschul, S. F., Gish, W., Miller, W., Myers, E. W., and Lipman, D. J. 1990. Basic local alignment search tool. J. Mol. Biol. 215:403-410.

Azad, H. R., Holmes, G. J., and Cooksey, D. A. 2000. A new leaf blotch disease of sudangrass caused by *Pantoea ananas* and *Pantoea stewartii*. Plant Dis. 84:973-979.

Bankevich, A., Nurk, S., Antipov, D., Gurevich, A. A., Dvorkin, M., Kulikov, A. S., Lesin, V. M., Nikolenko, S. I., Pham, S., Prjibelski, A. D., Pyshkin, A. V., Sirotkin, A. V., Vyahhi, N., Tesler, G., Alekseyev, M. A., and Pevzner, P. A. 2012. SPAdes: A new genome assembly algorithm and its applications to single-cell sequencing. J. Comput. Biol. 19:455-477.

Bomfeti, C. A., Souza-Paccola, A., Massola Júnior, N. S., Marriel, I. E., Meirelles, W. F., Casela, C. R., and Paccola-Meirelles, L. D. 2008. Localization of *Pantoea ananatis* inside lesions of maize white spot disease using transmission electron microscopy and molecular techniques. Trop. Plant Pathol. 33:63-66.

Cother, E. J., Reinke, R., McKenzie, C., Lanoiselet, V. M., and Noble, D. H. 2004. An unusual stem necrosis of rice caused by *Pantoea ananas* and the first record of this pathogen on rice in Australia. Australas. Plant Pathol. 33:495-503.

Delcher, A. L., Harmon, D., Kasif, S., White, O., and Salzberg, S. L. 1999. Improved microbial gene identification with GLIMMER. Nucleic Acids Res. 27:4636-4641.

Galkiewicz, J. P., and Kellogg, C. A. 2008. Cross-kingdom amplification using bacteria-specific primers: Complications for studies of coral microbial ecology. Appl. Environ. Microbiol. 74:7828-7831.

Gitaitis, R. D., and Gay, J. D. 1997. First report of leaf blight, seed stalk rot, and bulb decay of onion by *Pantoea ananas* in Georgia. Plant Dis. 81:1096.

Goszczynska, T., Botha, W. J., Venter, S. N., and Coutinho, T. A. 2007. Isolation and identification of the causal agent of brown stalk rot, a new disease of corn in South Africa. Plant Dis. 91:711-718.

Gotz, S., Garcia-Gomez, J. M., Terol, J., Williams, T. D., Nagaraj, S. H., Nueda, M. J., Robles, M., Talon, M., Dopazo, J., and Conesa, A. 2008. High-throughput functional annotation and data mining with the Blast2GO suite. Nucleic Acids Res. 36:3420-3435.

Gurevich, A., Saveliev, V., Vyahhi, N., and Tesler, G. 2013. QUAST: Quality assessment tool for genome assemblies. Bioinformatics (Oxford, England) 29:1072-1075.

Huerta-Cepas, J., Szklarczyk, D., Heller, D., Hernández-Plaza, A., Forslund, S. K., Cook, H., Mende, D. R., Letunic, I., Rattei, T., Jensen, L. J., Mering, C., and Bork, P. 2019. EggNOG 5.0: A hierarchical, functionally, and phylogenetically annotated orthology resource based on 5090 organisms and 2502 viruses. Nucleic Acids Res. 47:D309-D314.

Jones, P., Binns, D., Chang, H. Y., Fraser, M., Li, W., McAnulla, C., McWilliam, H., Maslen, J., Mitchell, A., Nuka, G., Pesseat, S., Quinn, A. F., Sangrador-Vegas, A., Scheremetjew, M., Yong, S. Y., Lopez, R., and Hunter, S. 2014. InterProScan 5: Genome-scale protein function classification. Bioinformatics 30:1236-1240.

Kearse, M., Moir, R., Wilson, A., Stones-Havas, S., Cheung, M., Sturrock, S., Buxton, S., Cooper, A., Markowitz, S., Duran, C., Thierer, T., Ashton, B., Mentjies, P., and Drummond, A. 2012. Geneious Basic: An integrated and extendable desktop software platform for the organization and analysis of sequence data. Bioinformatics 28:1647-1649.

Krawczyk, K., Foryś, J., Nakonieczny, M., Tarnawska, M., and Bereś, P. K. 2021. Transmission of *Pantoea ananatis*, the causal agent of leaf spot disease of maize (*Zea mays*), by western corn rootworm (*Diabrotica virgifera virgifera* LeConte). Crop Prot. 141:105431.

Krawczyk, K., Wielkopolan, B., and Obrępalska-Stęplowska, A. 2020. *Pantoea ananatis*, a new bacterial pathogen affecting wheat plants (*Triticum* L.) in Poland. Pathogens 9:1079.

Maniatis, T., Fritsch, E. F., and Sambrook, J. 1982. Molecular Cloning – A Laboratory Manual. Cold Spring Harbor Laboratory, Cold Springs Harbor, NY.

Obasa, K., and Haynes, L. 2022. Two bacterial pathogens of peanut, causing early seedling decline disease, identified in the Texas Panhandle. Plant Dis. 106:648-653.

Paccola-Meirelles, L. D., Ferreira, A. S., Meirelles, W. F., Marriel, I. E., and Casela, C. R. 2001. Detection of a bacterium associated with leaf spot disease of maize in Brazil. J. Phytopathol. 149:275-279.

Richter, M., Rosselló-Móra, R., Glöckner, F. O., and Peplies, J. 2015. JSpeciesWS: A web server for prokaryotic species circumscription based on pairwise genome comparison. Bioinformatics 32:929-931.

Roper, M. C. 2011. *Pantoea stewartii* subsp. *stewartii*: Lessons learned from a xylem-dwelling pathogen of sweet corn. Mol. Plant Pathol. 12: 628-637.

Serrano, F. B. 1928. Bacterial fruitlet brown-rot of pineapple in the Philippines. Philipp. J. Sci. 36:271-324.

Stall, R. E., Alexander, L. J., and Hall, C. B. 1969. Effect of tobacco mosaic virus and bacterial infections on occurrence of graywall of tomato (*Erwinia ananas*). Proc. Fla. State Hort. Soc. 81:157-161.

Tamura, K., and Nei, M. 1993. Estimation of the number of nucleotide substitutions in the control region of mitochondrial DNA in humans and chimpanzees. Mol. Biol. Evol. 10:512-526.